

Thermocapillary convection in a rectangular cavity under the influence of surface contamination

JYH-CHEN CHEN and SHIH-FAN KUAN

Department of Mechanical Engineering, National Central University, Chung-Li, Taiwan 32054, R.O.C.

(Received 12 August 1991 and in final form 10 December 1991)

Abstract—This study examines the influence of insoluble surfactant on the steady thermocapillary flow in a rectangular cavity with an upper, deformable free surface and differentially heated side walls. The numerical solutions are obtained with a finite difference method, together with a boundary-fitted curvilinear coordinate system. The results show that the thermocapillary convection can be stabilized by the addition of an insoluble surfactant. Furthermore, as the concentration of the surfactant increases (higher elasticity number), oscillatory instability caused by that surfactant may occur when the slope of the surface tension becomes negative. For higher Peclet numbers, the concentration boundary is formed near the cold wall, and the clean surface appears in the region near the hot wall. Oscillatory flow may also be induced by a high local surfactant concentration that is created by a concentration boundary.

1. INTRODUCTION

IT IS WELL KNOWN that bulk fluid motions may be induced by variations in surface tension at the interface between two fluids. Such surface tension variations may be caused by non-uniform distributions of surface temperature or concentration. Fluid motions due to temperature gradients are called ‘thermocapillary convection’. In recent years, interest in thermocapillary flows has arisen in connection with the production of high-quality materials. The importance of thermocapillary convection has been discussed by Ostrach [1].

The influence of surface contamination on thermocapillary convection is the subject of considerable study. Knowledge of this effect is important in practical situations, as the characteristics of resolidified material in a material process are usually influenced by the transport behavior of heat, momentum, and mass during the melting. It is difficult to analyze a problem that involves the heat, momentum, and mass transfer with an unknown gas–liquid interface. Homsy and Meiburg [2] have extended the asymptotic analysis of Shen and Davis [3] in studying the influence of surface contamination in a rectangular cavity. They simplified the mass transfer problem by assuming an insoluble surfactant absorbed at the gas–liquid interface. Two dimensionless parameters were introduced: a surface Peclet number Pe , which represents the ratio of the insoluble surfactant convection to diffusion, and an elasticity number E , which indicates the ratio of the variation in surface tension generated by the insoluble surfactant to that induced by the temperature difference. They showed that the thermocapillary convection strength is suppressed by

the addition of an insoluble surfactant, and for $E \ll 1$ and $Pe \gg 1$, sharp gradients in surfactant concentrations form near the cold wall. Carpenter and Homsey [4] considered the thermocapillary flow in a two-dimensional slot with the effect of a partially contaminated interface. They assumed that the free surface was non-deformable, and found that for $Pe \gg 1$ the region of surface stagnation depended on elasticity number E . The results of refs. [2–4] are valid for slow fluid motions in a shallow, two-dimensional cavity, but because the motion of flow occurring in the material process is very vigorous, an analysis without consideration of the effects of strong convection may be physically unrealistic. As mentioned by Berg and Acrivos [5], the convective instability can be stabilized by a surfactant. Therefore it is of interest to study the effect of surfactants on strong thermocapillary convection.

In order to gain further understanding of the effect of surface contamination on thermocapillary convection in a rectangular cavity, we have performed a series of numerical computations. The numerical technique, which is an extended version of that used previously by Chen *et al.* [6, 7], has been used to solve the non-linear governing equations. The results of these computations will be compared with previous asymptotic results.

2. MATHEMATICAL FORMULATION

The physical model consists of a rectangular cavity of height H and length L containing a Newtonian fluid of constant density ρ , dynamic viscosity μ , kinematic viscosity ν , thermal conductivity k , and thermal diffusivity α , as shown in Fig. 1. The temperatures at $x' = 0$

NOMENCLATURE

A	aspect ratio
c	dimensionless surface concentration
c'	surface concentration
c_0	average surface concentration
c_p	specific heat
Ca	capillary number
D	surface diffusion coefficient
E	elasticity number
h	location of the free surface
H	height of the cavity
L	length of the cavity
Ma	Marangoni number
p	dimensionless pressure
p'	pressure
Pe	Peclet number
Pr	Prandtl number
Re	Reynolds number
T	dimensionless temperature
T'	temperature
T_c	temperature at $x' = L$
T_h	temperature at $x' = 0$

u	dimensionless horizontal velocity
v	dimensionless vertical velocity
x	dimensionless horizontal coordinate
x'	horizontal coordinate
y	dimensionless vertical coordinate
y'	vertical coordinate.

Greek symbols

α	thermal diffusivity
γ_c	surface concentration coefficient
γ_T	surface tension temperature coefficient
μ	dynamic viscosity
ν	kinematic viscosity
ρ	density
σ	surface tension
σ_0	mean value of free surface
ψ	stream function
ω	vorticity.

Subscripts

x, y	derivative with respect to x, y .
--------	-------------------------------------

and $x' = L$ are T_h and T_c , respectively. The bottom surface is thermally insulated, while the top free surface is cooled by heat transfer to the gas. We assume that the free surface is contaminated by an insoluble surfactant. The surface tension is considered as a monotonically decreasing function of temperature and local surface concentration of the surfactant:

$$\sigma = \sigma_0 - \gamma_T(T' - T_0) - \gamma_c(c' - c_0) \quad (1)$$

where σ_0 is the mean surface tension at reference temperature $T_0 = (T_h + T_c)/2$ and average surface concentration c_0 , and the constants γ_T and γ_c represent the rate of surface tension change with respect to temperature and concentration, respectively.

Following Chen *et al.* [6], we introduce the following non-dimensional variables:

$$\begin{aligned} x &= x'/H, & y &= y'/H, & u &= u'/(\gamma\Delta T/\mu), \\ v &= v'/(\gamma_T\Delta T/\mu), & p &= p'/(\gamma_T\Delta T/H), & h &= h'/H, \\ T &= (T' - T_0)/\Delta T, & c &= c'/c_0, \end{aligned} \quad (2)$$

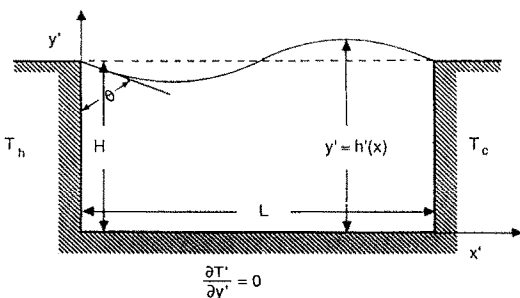


Fig. 1. Schematic diagram of the physical system.

where $\Delta T = T_h - T_c$. The dimensionless governing equations for the steady two-dimensional motion of the liquid are the following:

$$u_x + v_y = 0 \quad (3a)$$

$$Re(uu_x + vv_y) = -p_x + u_{xx} + u_{yy} \quad (3b)$$

$$Re(uv_x + vv_y) = -p_y + v_{xx} + v_{yy} \quad (3c)$$

$$Ma(uT_x + vT_y) = T_{xx} + T_{yy}. \quad (3d)$$

Here, the stream function ψ is given by:

$$u = \psi_y, \quad v = -\psi \quad (4)$$

and the vorticity is defined as:

$$\omega = v_x - u_y. \quad (5)$$

The two dimensionless parameters which appear in equations (3) are:

$$\text{Reynolds number, } Re = \gamma_T\Delta TH/\mu\nu,$$

$$\text{Marangoni number, } Ma = RePr = \gamma_T\Delta TH/\mu\alpha,$$

where Pr is the Prandtl number, ν/α .

Eliminating the pressure from equation (3), we obtain:

$$Re(\psi_y\omega_x - \psi_x\omega_y) = \omega_{xx} + \omega_{yy} \quad (6a)$$

$$Ma(\psi_yT_x - \psi_xT_y) = T_{xx} + T_{yy} \quad (6b)$$

$$-\omega = \psi_{xx} + \psi_{yy}. \quad (6c)$$

The appropriate boundary conditions are as follows:

$$\psi = T_y = 0, \quad \omega = -\psi_{xx}; \quad y = 0 \quad (7a-c)$$

$$\psi = 0, \quad \omega = -\psi_{xx}, \quad T = 1/2; \quad x = 0 \quad (8a-c)$$

$$\begin{aligned}
\psi &= 0, \quad \omega = -\psi_{xx}, \quad T = -1/2; \quad x = 1/A \quad (9a-c) \\
\psi &= 0, \\
-p + 2(1+h_x^2)^{-1}[-\psi_{xy} - \psi_{yy}h_x + h_x(\psi_{xy}h_x + \psi_{xx})] &= \\
Ca^{-1}h_{xx}(1+h_x^2)^{-3/2}(1-CaT-ECa(c-1)), & \\
(1-h_x^2)\omega = (1+h_x^2)^{1/2}(T_x+h_xT_y+Ec_x) & \\
-2\psi_{xx}(1-h_x^2)-4h_x\psi_{xy}, & \\
(1-h_x^2)^{-1}(T_y-T_xh_x) = Bi(T+Ax-1/2), & \\
c_{xx}-h_xh_{xx}(1-h_x^2)^{-1}c_x = APe(1+h_x^2) & \\
\times [(\psi_y,c)_x - \psi_ych_xh_{xx}(1-h_x^2)^{-1}]; \quad y = h(x). & (10a-e)
\end{aligned}$$

The boundary conditions contain five dimensionless parameters: aspect ratio $A = H/L$, capillary number $Ca = \gamma_T \Delta T / \sigma_0$, elasticity number $E = c_0 \gamma_c / (\gamma_T \Delta T)$, surface Peclet number $Pe = \gamma_T \Delta T L / (\mu D)$ and Biot number $Bi = hH/k$, where D is the surface diffusion coefficient and h is the surface heat transfer coefficient. Equation (10a) expresses the kinematic condition on the free surface. Equations (10b)–(10d) represent the normal and shear-stress balances and the thermal condition. Following Levich [8], the convection of an insoluble surfactant along the free surface is expressed by equation (10e).

Since the liquid volume and the total surface concentration remain constant:

$$\int_0^{1/A} h(x) dx = \frac{1}{A} \quad (11a)$$

$$\int_0^{1/A} c(x) dx = \frac{1}{A}. \quad (11b)$$

The contact line conditions are restricted to the case of the liquid sticking to the sharp edge at the solid end walls,

$$h(0) = h(1/A) = 1, \quad (12)$$

and the concentration gradient is assumed to be zero at the solid end walls,

$$c_x(0) = c_x(1/A) = 0. \quad (13)$$

The finite difference scheme originally developed by Chen *et al.* [6] to study thermocapillary convection in a rectangular cavity has been modified to solve system (6) with conditions (7)–(13). The discrete form of the system is constructed using second-order central differencing. The calculations are initiated by assigning an initial shape to the gas–liquid interface. A boundary-fitted curvilinear coordinate system [9] has been generated that has coordinate lines that coincide with the current boundary. Grid-stretching transformation has been employed to provide good resolution near the gas–liquid interface. Initial guesses for ψ , ω , and T over the entire computation domain were chosen. The difference equation for ω is solved using these initial guesses to form the non-linear term in equation (6a) and boundary conditions (7)–(9) and (10c). After the new ω is obtained, the difference equations for ψ

and T are solved iteratively using the successive-line-overrelaxation (SLOR) method. The new solutions for ψ and T are used to correct the initial guesses for ψ and T , and the procedure is repeated until the relative error of two subsequent computations is within a specified limit, generally taken as 10^{-4} . The surfactant equation (10e) is solved using the shooting method. Then the normal-stress condition (10b) is checked. If that condition is not satisfied, the gas–liquid interface is modified to reduce the difference; the complete discussion of the search procedure for the new interface shape is described in detail in ref. [6] and is therefore not repeated here. With a new interface shape, we repeat the solution procedure discussed above until all equations and boundary conditions are satisfied.

3. RESULTS AND DISCUSSION

The numerical computations described in the previous section were done on the National Central University VAX 8650 computer using double-precision arithmetic. Computations were performed for cases in which the aspect ratio was 0.2, the Prandtl number was 10, and the Biot number was 1. The total number of mesh points was chosen from 41×41 to 201×41 , depending on the Marangoni number Ma ; 41×41 for $Ma = 10$, 81×41 for $Ma = 500$, and 201×41 for $Ma = 5000$.

The influences of the elasticity and Peclet numbers on the surface deformation have been considered. Figure 2 shows the free-surface shape for $Ma = 10$, $Pe = 100$, and $Ca = 0.1$ with different E , while Fig. 3

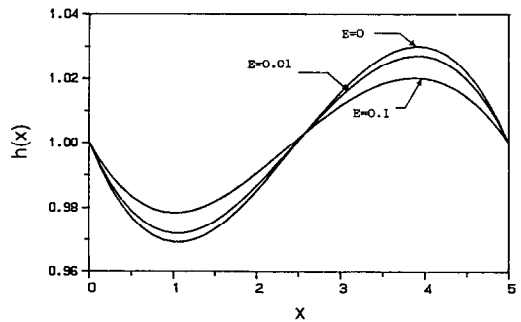


FIG. 2. The interface shape for $Ma = 10$, $Pe = 100$, and $Ca = 0.1$ with different E .

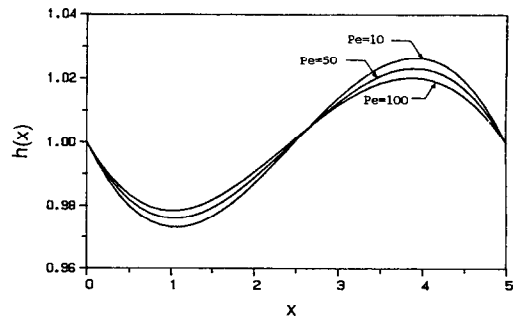


FIG. 3. The interface shape for $Ma = 10$, $Pe = 0.1$, and $Ca = 0.1$ with different Pe .

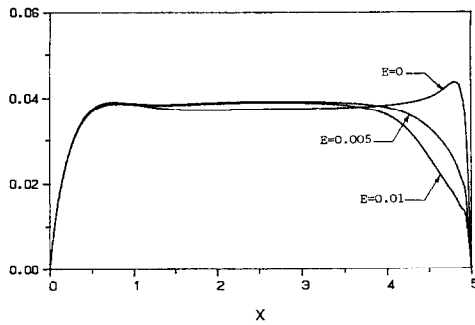


FIG. 4. The distribution of surface velocity for $Ma = 500$, $Pe = 1000$, and $Ca = 0.02$ with different E .

illustrates the interface shape for $Ma = 10$, $E = 0.1$, and $Ca = 0.1$ with different Pe . The amount of surface deflection decreases as E and Pe increase. The surface deflections for small parameters are in qualitative and quantitative agreement with those of Homsy and Meiburg [2].

Figures 4 and 5 illustrate the effect of the elasticity and Peclet numbers on the surface velocity. It is clear that the present results are consistent with those of the asymptotic results [2] in that the surface velocity decreases as the elasticity and Peclet numbers increase. The influences of E and Pe are more significant near the cold region. In the cavity, the flow motion induced by the temperature gradient is clockwise, where the fluid is driven from the hot side to the cold side near the gas-liquid interface and moves back near the bottom wall [6]. The surfactant concentration near the cold side is much richer than it is near the hot side because the surfactant has shifted to the cold side due to the clockwise flow motion. Hence, the magnitude of surface velocity is more significantly reduced by the surfactant near the cold region. For higher E , the influence of the surfactant on the surface tension is more significant than the temperature difference. Also, the distribution of surfactant is more non-uniform for higher Pe (Fig. 8). These are the reasons for the decrease of surface velocity near the cold wall for higher E and Pe . Based on the stability analysis of Smith and Davis [10, 11], it is to be expected that unsteady thermocapillary motions will occur above

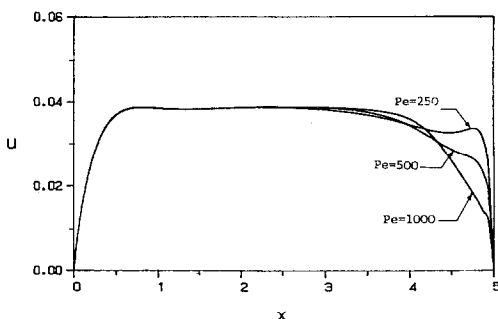


FIG. 5. The distribution of surface velocity for $Ma = 500$, $E = 0.01$, and $Ca = 0.02$ with different Pe .

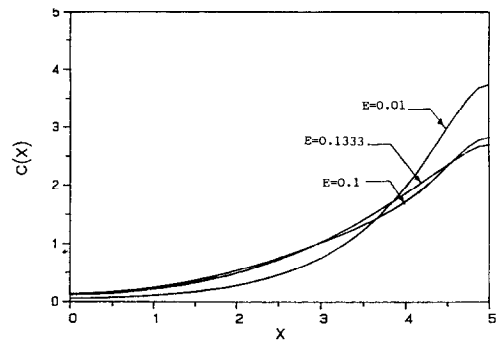


FIG. 6. The distribution of surfactant concentration for $Ma = 10$, $Pe = 100$, and $Ca = 0.1$ with different E .

some critical Ma . As mentioned by Zebib *et al.* [12], the peak velocity near the cold region is the major cause for the instability of thermocapillary convection. One may conjecture that the thermocapillary flow is stabilized by the addition of an absolute surfactant.

Figure 6 shows the influence of E on the surfactant concentration. For smaller E , the surface tension gradient is mainly induced by the temperature gradient. The high local concentration is formed near the cold region resulting from the convection effect due to thermocapillary flow motion. The local surface tension strength decreases as the concentration of insoluble surfactant increases because the shear stress caused by the concentration is in opposition to the thermocapillary stress. Therefore, increasing E results in a reduction of the convection effect due to thermocapillary flow motion. This is the reason why the surfactant concentration is more uniform for higher E . Figure 7 illustrates the distribution of surface tension gradient for $Ma = 10$, $Pe = 100$, and $Ca = 0.1$ with different E . From Fig. 5, it is clear that the surface tension gradient decreases with increasing E , especially for the region near the cold wall. For $E = 0.1333$, the surface tension gradient at $x = 4.5$ is almost zero. When $E > 0.14$, it is obvious that a negative surface tension gradient may appear. In our computations, a convergent solution cannot be obtained beyond this value, possibly because the surface tension gradient near the cold wall oscillates from the

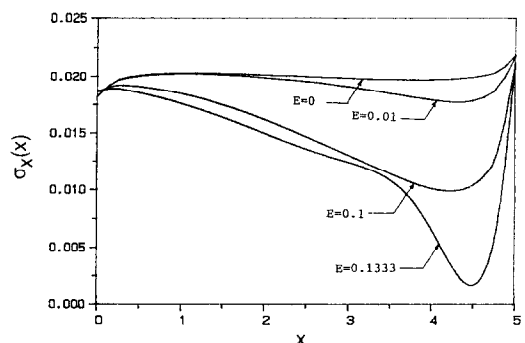


FIG. 7. The distribution of surface tension gradient for $Ma = 10$, $Pe = 100$, and $Ca = 0.1$ with different E .

negative value to the positive value. When the negative surface tension gradient occurs, a stagnant point is formed at the free surface and the flow motion in the cavity is separated into two regions: a clockwise motion near the hot wall and an anti-clockwise motion near the cold wall. The negative surface tension gradient will change to the positive value because the anti-clockwise flow motion will drive the insoluble surfactant from the low temperature region to the high temperature region. The positive surface tension gradient will switch back to the negative value due to the clockwise flow motion. Therefore, an oscillatory motion may be established when E is greater than this critical value. This implies that the zero surface tension gradient could be the criterion for the onset of the oscillatory instability caused by the insoluble surfactant. Of course, this must be verified by further experiments and stability studies. The critical elasticity number decreases with increasing Ma , Pe and Ca . For $Ma = 5000$ and $Pe = 1000$, the critical elasticity number is around 0.006.

Figure 8 shows the effect of Pe on the surface concentration. From Fig. 8, we can see that the surface concentration is nearly constant for $Pe = 10$, and the concentration boundary layer is formed near the cold wall with further increases in Pe . When Pe exceeds a certain critical value, the clean surface appears in the region near the hot wall. The extent of the clean surface increases with continuous increases in Pe . We choose to define the clean length x_c as the length of the surface where $c(x) < 0.01$. Figure 9 demonstrates that for a fixed Pe , x_c increases with increasing Re , and for a fixed Ma , x_c increases exponentially for smaller Pe and asymptotically for higher Pe . In Fig. 9, a convergent solution will not be obtained when $x_c > 4.1$ for $Ma = 100$ and $x_c > 4.25$ for $Ma = 5000$. This may be caused by the appearance of a negative surface tension gradient resulting from a high local surfactant concentration near the cold region. Therefore, the transient flow motion may be generated by the strong surfactant convection.

4. CONCLUSION

Numerical computations have been performed to study the influence of an insoluble surfactant on the

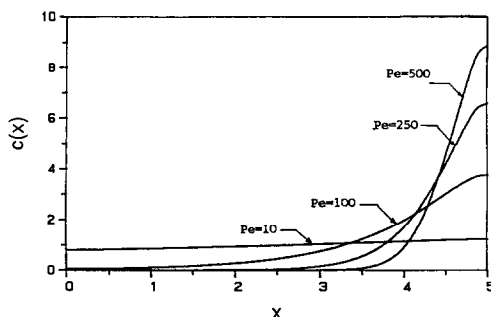


FIG. 8. The distribution of surface concentration for $Ma = 10$, $E = 0.01$, and $Ca = 0.1$ with different Pe .

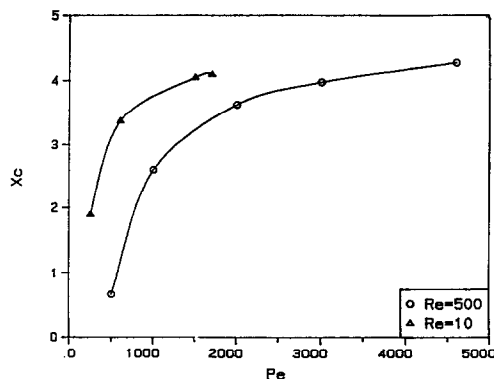


FIG. 9. Clean length x_c vs Pe for $E = 0.005$ and $Ca = 0.001$ with $Re = 10$ and 500.

thermocapillary convection in a rectangular cavity. The results show that the thermocapillary flow may be stabilized by the addition of an insoluble surfactant. The strength of the thermocapillary flow is reduced with increasing E or Pe . With further increases in E or Pe , oscillatory flow may occur due to the appearance of a negative surface tension gradient caused by the insoluble surfactant. The magnitude of the critical elasticity number decreases with increasing Ma , Pe and Ca . The clean surface forms the region near the hot wall when Pe exceeds a certain critical value, and the region of clean surface increases when Re increases.

Acknowledgement—This research was supported by the National Science Council of R.O.C. under Grant No. NSC79-0401-E-008-17.

REFERENCES

1. S. Ostrach, Low-gravity fluid flows, *A. Rev. Fluid Mech.* **14**, 313–345 (1982).
2. G. M. Homsy and E. Meiburg, The effect of surface contamination on thermocapillary flow in a two-dimensional slot, *J. Fluid Mech.* **139**, 443–459 (1984).
3. A. K. Shen and S. H. Davis, Steady thermocapillary flows in two-dimensional slots, *J. Fluid Mech.* **121**, 163–186 (1982).
4. B. Carpenter and G. M. Homsy, The effect of surface contamination on thermocapillary flow in a two-dimensional slot. Part 2. Partially contaminated interfaces, *J. Fluid Mech.* **155**, 429–439 (1985).
5. J. C. Berg and A. Acrivos, The effect of surface agents on convection rolls induced by surface tension, *Chem. Engng Sci.* **20**, 737–745 (1965).
6. J. C. Chen, J. C. Sheu and S. S. Jwu, Numerical computation of thermocapillary convection in a rectangular cavity, *Numer. Heat Transfer* **17A**, 287–308 (1990).
7. J. C. Chen, J. C. Sheu and Y. T. Lee, Maximum stable length of nonisothermal liquid bridges, *Physics Fluids* **2A**, 1118–1123 (1990).
8. V. G. Levich, *Physicochemical Hydrodynamics*. Prentice-Hall, Englewood Cliffs, NJ (1962).
9. J. F. Thompson, F. C. Thames and W. Mastin, Automatic numerical generation of body fitted curvilinear coordinate system for field containing any number of

- arbitrary two-dimensional bodies, *J. Comput. Phys.* **15**, 299–319 (1974).
10. M. K. Smith and S. H. Davis, Instabilities of dynamic thermocapillary liquid layers. Part 1. Convective instabilities, *J. Fluid Mech.* **132**, 119–144 (1983).
11. M. K. Smith and S. H. Davis, Instabilities of dynamic thermocapillary liquid layers. Part 2. Surface-wave instabilities, *J. Fluid Mech.* **132**, 145–162 (1983).
12. A. Zebib, G. M. Homsy and E. Meiburg, High Marangoni number convection in a square cavity, *Physics Fluids* **12**, 3367–3376 (1986).

CONVECTION THERMOCAPILLAIRE DANS UNE CAVITE RECTANGULAIRE SOUS L'INFLUENCE DE LA CONTAMINATION DE LA SURFACE

Résumé—On examine l'influence d'un surfactant insoluble sur l'écoulement permanent thermocapillaire dans une cavité rectangulaire avec une surface supérieure librement déformable et des parois latérales chauffées différemment. Les solutions numériques sont obtenues par une méthode aux différences finies avec un système de coordonnées curvilignes. Les résultats montrent que la convection thermocapillaire peut être stabilisée par l'addition d'un surfactant insoluble. Lorsque la concentration du surfactant augmente (nombre d'élasticité plus élevé), l'instabilité oscillatoire causée par ce surfactant peut se produire si la pente de la tension superficielle devient négative. Pour des nombres de Péclet élevés, la couche de concentration est formée près de la surface froide et la surface propre apparaît dans la région proche de la paroi chaude. Un écoulement oscillatoire peut aussi être induit par une concentration locale très élevée de surfactant qui est créée par une couche de concentration.

THERMOKAPILLARE KONVEKTION IN EINEM RECHTECKIGEN HOHLRAUM UNTER DEM EINFLUSS VON OBERFLÄCHENVERUNREINIGUNGEN

Zusammenfassung—In der vorliegenden Arbeit wird der Einfluß von nichtlöslichen oberflächenaktiven Stoffen auf die gleichmäßige thermokapillare Strömung in einem rechteckigen Hohlraum mit einer deformierbaren freien Oberfläche und unterschiedlich beheizten Seitenwänden untersucht. Die numerischen Lösungen werden mit einem Finite-Differenzen-Verfahren zusammen mit einem oberflächenangepaßten gekrümmten Koordinatensystem bestimmt. Die Ergebnisse zeigen, daß die thermokapillare Konvektion durch Zugabe eines nichtlöslichen oberflächenaktiven Stoffes stabilisiert werden kann. Weiterhin kann bei steigender Konzentration des oberflächenaktiven Stoffes (Höhere Elastizitäts-Zahl) eine oszillatorische Instabilität durch diesen oberflächenaktiven Stoff hervorgerufen werden, wenn die Steigung der Oberflächenspannung negativ wird. Für höhere Peclet-Zahlen bildet sich die Konzentrationsgrenzfläche in der Nähe der kalten Wand, und die reine Oberfläche erscheint nahe der heißen Wand. Oszillatorische Strömungen können auch durch hohe örtliche Konzentration des oberflächenaktiven Stoffes an einer begrenzenden Fläche hervorgerufen werden.

ТЕРМОКАПИЛЛЯРНАЯ КОНВЕКЦИЯ В ПОЛОСТИ ПРЯМОУГОЛЬНОГО СЕЧЕНИЯ ПОД ВЛИЯНИЕМ ЗАГРЯЗНЕНИЯ ПОВЕРХНОСТИ

Аннотация—Исследуется влияние нерастворимого ПАВ на стационарное термокапиллярное течение в полости прямоугольного сечения с деформируемой свободной верхней поверхностью и локально нагреваемыми боковыми стенками. Численные решения получены с использованием конечно-разностного метода и криволинейной системы координат, связанной с границей. Результаты показывают, что термокапиллярная конвекция может стабилизироваться посредством добавления нерастворимого ПАВ, а с дальнейшим увеличением концентрации ПАВ может возникнуть колебательная неустойчивость, когда наклон поверхностного натяжения становится отрицательным. При высоких числах Пекле возле ненагретой стенки образуется концентрационная граница, а в области у нагретой стенки появляется чистая поверхность. Колебательное течение может также обуславливаться высокой локальной концентрацией ПАВ, создаваемой концентрационной границей.